Li-Qiang Feng* and Li Liu

Control of the half-cycle harmonic emission process for generating the intense and ultrashort single attosecond pulses (SAPs)

https://doi.org/10.1515/zna-2020-0170 Received June 28, 2020; accepted August 4, 2020; published online September 7, 2020

Abstract: In this paper, the half-cycle harmonic generation process has been controlled by using the asymmetric inhomogeneous chirped pulse combined with the ultraviolet (UV) pulse. It is found that by properly optimizing the chirps and chirp delays of the fundamental two-color pulse, the optimal negative and positive half-cycle laser profiles for the harmonic cutoff extension can be obtained. Further, with the introduction of the negative and positive inhomogeneous effect, respectively, the harmonic cutoff from the negative and positive half-cycle laser profiles can be further improved. Next, with the assistance of the UV pulse, the harmonic intensity can be enhanced due to the UV resonance ionization. Moreover, the single and double UV photon resonance ionizations are much better for generating the higher harmonic intensity. As a result, the stronger and broader harmonic plateaus with the larger harmonic cutoff can be obtained, which can support the generation of the high-intensity ultrashort attosecond pulses with the pulse durations of sub-45 as.

Keywords: half-cycle harmonic emission process; highorder harmonic generation; inhomogeneous laser field; multicolor combined field; single attosecond pulse.

1 Introduction

Fascinating developments of the ultrafast optics have stimulated the generation of attosecond pulses in the extreme ultraviolet (XUV) and even in the soft X-ray regimes. These lights provide the possibility to probe and study the ultrafast processes with the unprecedented resolutions [1–3]. Due to the unique harmonic spectral plateau structure, the high-

*Corresponding author: Li-Qiang Feng, Laboratory of Molecular Reaction Dynamics, Liaoning University of Technology, Jinzhou, 121001, China, E-mail: lqfeng_lngy@126.com
Li Liu, General Technology Group Dalian Machine Tool Co., Ltd, Dalian, 116600, China

order harmonic generation (HHG) spectrum is the only effective method to realize the single attosecond pulses (SAPs) [4–6]. Generally, the HHG spectrum can be obtained when the intense laser fields interact with atoms, molecules and solids [7–10]. Although, the attosecond pulses can be produced from the above three kinds of HHG spectra, the most successful and effective method to produce the SAPs is still the HHG from atoms.

Specifically, the HHG from atoms (especially for the noble gases) has been well explained by Corkum [11] with the model of 'ionization-acceleration-recombination' in each half-cycle laser profile, which is called the three-step model. In the 1st step of ionization process, the electron is tunnel-ionized from the Coulomb potential. In the 2nd step of acceleration process, the electron can gain the kinetic energy in the following half-cycle laser profile. In the 3rd step of recombination process, the electron recombines with its parent atom and releases photon with the photon energy equaling to the sum of the ionization potential of atom and the obtained kinetic energy of the electron. Finally, by superposing some harmonics on the spectral continuum, the SAPs can be obtained.

Based on the three-step model, the harmonic intensity is mainly dependent on the ionization process and the harmonic cutoff is sensitive to the acceleration process [11]. Thus, controlling the half-cycle harmonic emission process is very important to obtain the intense and broad spectral continuum. For instance, in the case of controlling the ionization process, by properly (1) using the high Rydberg initial state [12, 13], (2) using the superposition of the initial state [14, 15] or (3) adding the ultraviolet (UV) pulse [16, 17], the ionization probability of the atomic system can be increased, which will lead to the intensity enhancement of the harmonic yield. Furthermore, in the other investigations, by using the charge resonance enhanced ionization scheme, the harmonic intensities of H₂⁺ and its isotope molecules can also be enhanced [18-20]. In the case of controlling the acceleration process, by using (1) the multicolor laser beams [21-25], (2) the frequency chirping technology [26–29], (3) the polarization gating technology [30–32] and (4) the inhomogeneous laser field [33–37], the broad harmonic plateau with the larger harmonic cutoff can be produced.

As can be seen, to produce the stronger and broader harmonic spectral plateau with the larger harmonic cutoff, both controlling the ionization and acceleration processes are requirement. However, in most of the former investigations, the controlling ionization and acceleration processes are separated. Thus, either the broader harmonic spectral plateau with the lower harmonic intensity can be obtained, or the stronger harmonic intensity with the narrow harmonic plateau and the smaller harmonic cutoff can be generated. Thus, in this paper, we propose an effective method to control the half-cycle harmonic emission process. Under this scheme, the ionization and acceleration processes can be controlled simultaneously. The controlling process can be separated into three parts. In the first process, with the introduction of the chirp and chirp delay of the two-color pulse (TCP), the optimal harmonic extension from the negative and positive half-cycle laser profiles can be obtained. In the second process, by properly adding the asymmetric inhomogeneous effect, the harmonic cutoffs from the negative and positive half-cycle laser profiles can be further extended. In the third process, with the assistance of the UV resonance ionization, the harmonic intensity can be remarkably improved with the introduction of a proper UV pulse. As a result, the stronger and broader harmonic plateau with the larger harmonic cutoff can be found, which can lead to the generation of the intense SAPs shorter than 45 as.

2 Methods

The time-dependent Schrödinger equation of He atom with the singleelectron approximation is given by [38-45],

$$i\frac{\partial\psi(x,t)}{\partial t} = \left[-\frac{1}{2}\frac{d^2}{dx^2} + V(x) + xE(t)\right]\psi(x,t),\tag{1}$$

where, $V(x) = -\frac{1}{\sqrt{0.080 + x^2}}$ is the Coulomb potential of He atom. Here, when the above potential model is used, the energies of the ground state and the first excited state of He atom are 24.56 and 4.68 eV, respectively, which are closed to the experimental date of 24.6 and 4.8 eV. E(t) is the laser field, which will be specifically described in discussion part.

The HHG spectrum $S(\omega)$ is given by,

$$S(\omega) = \left| \frac{1}{\sqrt{2\pi}} \int a(t)e^{-i\omega t} dt \right|^2, \tag{2}$$

where, $a(t) = \langle \psi(x,t) | -\frac{\partial V(x)}{\partial x} + E(t) | \psi(x,t) \rangle$. The time profile of HHG is given by [46],

$$A(t,\omega) = \int a(t')\sqrt{\omega}W(\omega(t'-t))dt', \tag{3}$$

where,
$$W(x) = \left(\frac{1}{\sqrt{\xi}}\right) e^{ix} e^{-x^2/2\xi^2}$$
.

The time profile of SAP is given by,

$$I_{\text{SAP}}(t) = \left| \sum_{q} \left(\int a(t) e^{-iq\omega t} dt \right) e^{iq\omega t} \right|^{2}$$
 (4)

The detail numerical method and process can be found in [38].

3 Results and discussion

3.1 Control of the acceleration process for the harmonic cutoff extension

The two-color fundamental pulse used in this paper is 20 fs-1600 nm and 10 fs-800 nm pulses with laser intensities being 0.5×10^{14} W/cm². The TCP can be expressed

$$E_{\text{TCP}}(t) = E_{1} \exp\left[-4\ln(2)t^{2}/\tau_{1}^{2}\right] \cos\left(\omega_{1}t + c_{1}\left(t - t_{\text{delay-}c1}\right)^{2}\right) + E_{2} \exp\left[-4\ln(2)t^{2}/\tau_{2}^{2}\right] \cos\left(\omega_{2}t + c_{2}\left(t - t_{\text{delay-}c2}\right)^{2}\right).$$
(5)

Here, $E_{1,2}$, $\omega_{1,2}$, $\tau_{1,2}$, $c_{1,2}$ and $t_{\text{delay}-c1,2}$ are the laser amplitudes, the laser frequencies, the pulse durations, the chirp parameters and the chirp delays of the TCP.

Figures 1(a) and 1(b) show the chirp effects on the harmonic cutoff extension. The chirp delays are zero. Firstly, for the case of c_1 , it is found that when $-8 \times 10^{-4} < c_1 < -6 \times 10^{-4}$, the harmonic cutoff is increases; while, as c_1 further moves to the positive value, the harmonic cutoff is decreased (see Figure 1(a)). Thus, $c_1 = -6$ is good for extending the harmonic cutoff. Here, it should be noted that the values of the chirps are very small (i.e. 10^{-4}). Thus, for convenience, the following order of magnitudes are omitted (i.e. $c_1 = -6 \times 10^{-4}$ is defined as $c_1 = -6$). Moreover, it should be illustrated that the units of the chirp parameters $c_{1,2}$ are rad/s². However, for convenience, the units of the chirp parameters are also omitted in the following discussion. Next, we see the effect of c_2 on the harmonic cutoff extension. Here, c_1 is chosen to be -6. It shows that when $c_2 = -8$ or $c_2 = -7$, the largest harmonic cutoff can be found; while, as c_2 moves to positive value, the harmonic cutoff is decreased first, and then it is increased again (see Figure 1(b)). However, the harmonic cutoffs are all smaller than that from $c_2 = -7$. Thus, $c_1 = -6$ and $c_2 = -7$ are the proper chirp combination for the harmonic cutoff extension. To better see the harmonic characteristics, in Figure 1(c), we present the HHG spectra of the chirp-free pulse ($c_1 = c_2 = 0$) and chirped pulse ($c_1 = -6$, c_2 = -7). Clearly, with the introduction of the chirp modulation, the harmonic cutoff can be remarkably extended; however, the harmonic intensity is decreased compared

with that from the chirp-free pulse. So, the harmonic enhancement is necessary and it will be discussed in the following part.

Figure 2 shows the laser profiles and the time profiles of HHG for the cases of the chirp-free pulse $(c_1 = c_2 = 0)$ and the above chirped pulse ($c_1 = -6$, $c_2 = -7$). Here, the units of the harmonic intensity used in the following color figures are "arb.units" and they are on a log scale. On the basis of the three-step model, the HHG occurs in each half-cycle laser profile. For the present two-color chirp-free pulse, there are many half-cycle laser profiles and the profile structure is much more complicated compared with the normal singlecolor laser field. However, due to the lower intensity on the rising and falling parts of the laser field, we only discuss the laser profiles in the middle amplitude regions. Clearly, there are four half-cycle laser profiles, marked as $A_{1\sim4}$, as shown in Figure 2(a). Based on the three-step model, these four half-cycle laser profiles will lead to four harmonic emission peaks (HEPs), marked as $P_{1\sim4}$, as shown in Figure 2(b). Moreover, we see that the intensity of P_4 is much higher than those of $P_{1\sim3}$ due to the sufficient ionization on the falling part of the laser field. With the introduction of the chirp modulation, the waveform of A_4 is broadened in comparison with the chirp-free pulse case. Thus, the electron will receive more energy when it accelerates in this waveform, which can lead to the extension of P_4 , as shown in Figure 2(c). This is also the reason behind the chirp effect on the harmonic cutoff extension. Through analyzing the laser profile and the time-profile of HHG, we see that for the case of the chirp-free pulse, the harmonic spectral region is coming from the multi-HEPs (see Figure 2(b)), thus, the higher harmonic intensity can be obtained. For the case of the chirped pulse, when the harmonics are lower than 100th order, the spectral region

is coming from many HEPs (see Figure 2(c)), thus leading to the comparable harmonic intensity of this spectral region compared with the chirp-free pulse case. While, when the harmonics are higher than 100th order, the higher harmonic spectral plateau is only coming from P_4 , which leads to the lower harmonic intensity in the higher spectral region and is responsible for the decrease of the harmonic intensity as the harmonic cutoff extension. Moreover, the higher harmonic spectral region, contributed by the single P_4 , is caused by the negative half-cycle laser profile of A_4 . For convenience, we define the laser profile with $c_1 = -6$, $c_2 = -7$ and $t_{\rm delay-c1} = t_{\rm delay-c2} = 0$ as the negative half-cycle profile in the following discussion.

We see that with the introduction of the chirps, the optimal harmonic extension from the negative half-cycle laser profile can be obtained. However, the HHG can be produced not only from the negative laser profile but also from the positive laser profile. Thus, in the next step, we try to find the optimal positive half-cycle laser profile for the harmonic extension. We know that there are many methods can change the laser profile. However, we want to obtain the laser profile based on the present two-color chirped pulse. So, we fix the chirp parameters of the TCP and only modulate the chirp delays to find the positive laser profile. Through our calculations, the chirp delays of the TCP should chosen to be $t_{\text{delay-}c1} = -0.6T$ and $t_{\text{de-}}$ $lav-c^2 = -0.3T$. Here, T is the optical cycle of 1600 nm pulse. As can be seen in Figure 3(a), by properly choosing the chirp delays of the TCP, a broader positive half laser waveform from t = 0 to t = 1.5T can be found, marked as A_5 . Thus, when the electron is ionized around t = 0, it will be accelerated in this positive half laser waveform, which can obtain the extra energy due to the longer accelerated time. As a result, the larger emitted photon energy can be found

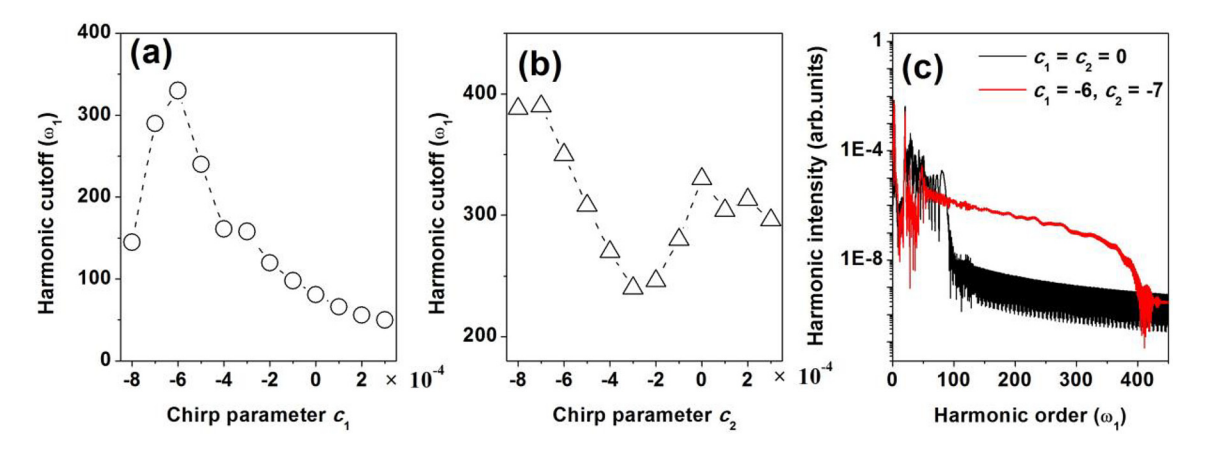


Figure 1: The chirp parameter effects on the harmonic cutoff (a) c_1 and (b) c_2 . (c) The harmonic spectra of $c_1 = c_2 = 0$ and $c_1 = -6$, $c_2 = -7$. The two-color pulse is 20 fs-1600 nm and 10 fs-800 nm with laser intensities being 0.5×10^{14} W/cm². The chirp delays are zero.

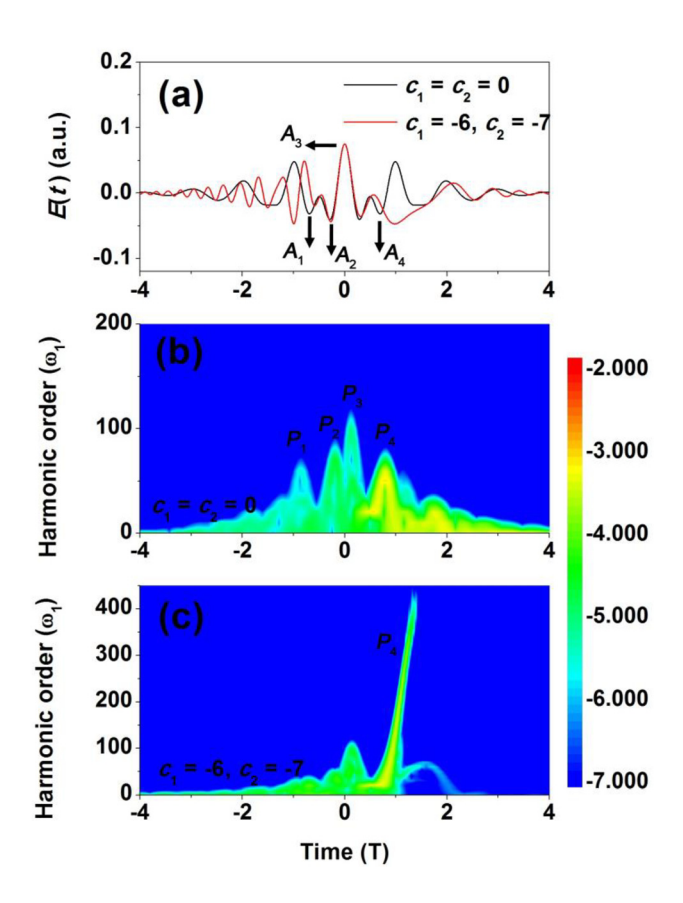


Figure 2: (a) The laser profiles of chirp-free ($c_1 = c_2 = 0$) and chirped pulse ($c_1 = -6$, $c_2 = -7$). The time-profiles of high-order harmonic generation (HHG) for the cases of (b) of $c_1 = c_2 = 0$ and (c) $c_1 = -6$, $c_2 = -7$. Here, the laser profile of $c_1 = -6$, $c_2 = -7$, $t_{\text{delay-c1}} = t_{\text{delay-c2}} = 0$ is called the negative half-cycle profile in the following discussion.

from the HEP of P_5 , as shown in Figure 3(b). This modulation can also lead to the extension of the harmonic cutoff, as shown in Figure 3(c). Moreover, the larger photon harmonic plateau region (i.e. the harmonic order is higher than 100th order) is only coming from P_5 , and it is caused by the positive half laser waveform of A_5 . Here, in the following discussion, we define the laser profile of $c_1 = -6$, $c_2 = -7$, $t_{\text{delay}-c1} = -0.6$ T and $t_{\text{delay}-c2} = -0.3$ T as the positive half-cycle profile.

For now, we get the optimal harmonic extension cases for the negative and positive half-cycle laser profiles. In the next step, we try to further extend the harmonic cutoff. As discussed before, there are many methods can extend the harmonic cutoff. For instance, either by increasing the laser intensity, or adding the controlling pulse, the harmonic cutoff can be extended. However, if the above two methods are chosen, although the harmonic cutoff can be extended, the harmonic structure will also be changed. Here, we only want to extend the HEP of P_4 and P_5 for the negative and positive laser profiles, respectively. Currently, the asymmetric inhomogeneous laser field is a proper method to

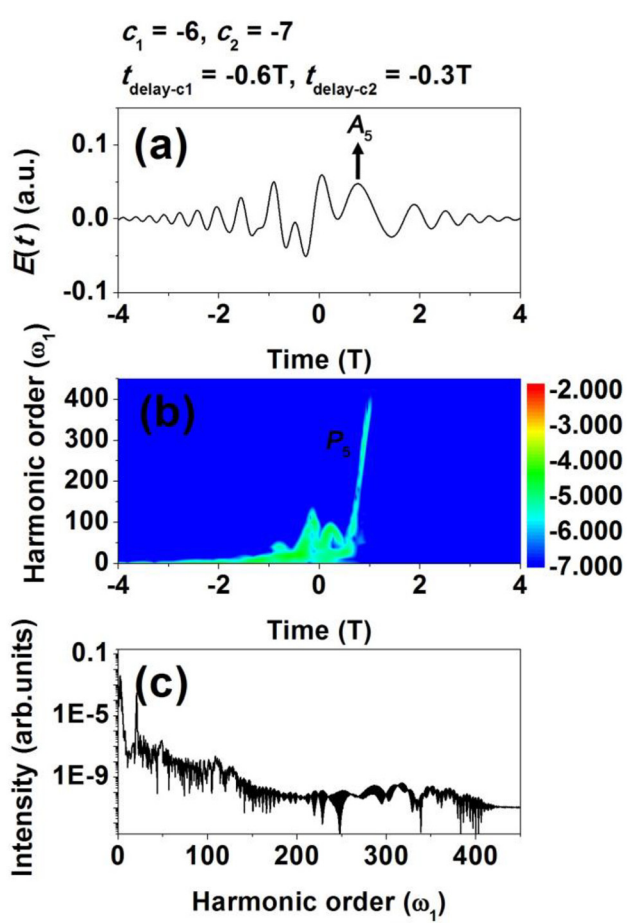


Figure 3: (a) The laser profile of chirped pulse with $c_1 = -6$, $c_2 = -7$, $t_{\rm delay-c1} = -0.6 T$ and $t_{\rm delay-c2} = -0.3 T$. (b) The time profile of highorder harmonic generation (HHG) driven by the above chirped pulse. (c) The HHG spectrum driven by the above chirped pulse. Here, the laser profile of $c_1 = -6$, $c_2 = -7$, $t_{\rm delay-c1} = -0.6 T$ and $t_{\rm delay-c2} = -0.3 T$ is called the positive half-cycle profile in the following discussion.

achieve this goal [33–37]. This is because that the laser intensity of the inhomogeneous field can be increased as the spatial extension. And the higher laser intensity can be found along the negative and positive electron motion direction for the cases of the negative and positive inhomogeneous fields, respectively. As a result, the electron will obtain more energy along its accelerated direction, which results in the extension of HEP [37]. Here, the inhomogeneous field is defined as $E(x, t) = (1 + \beta x)E(t)$, where β is the inhomogeneous parameter with $\beta < 0$ and $\beta > 0$ meaning the negative and positive inhomogeneous fields, respectively. In the present paper, we choose $\beta = \pm 0.001$ as the inhomogeneous parameters. Here, we briefly introduce the experimental setup of the inhomogeneous field. The geometry of the metallic nanostructure is chosen to be the bow-tieshaped nanostructure [33]. The antenna is formed by two identical triangular gold pads separated by an air gap g, as

shown in Figure 4. The apices at corners were rounded (10 nm radius of curvature) to account for limitation of current fabrication techniques and avoid nonphysical fields enhancement due to tip-effect. The out of plane thickness is set to 25 nm [47]. Here, we take the field enhancement along the main axis passing through the apices and the electron motion of the He atom is adjusted as to coincide with this axis and centroid coordinates with the gap center. The present inhomogeneous parameters of $\beta = \pm 0.001$ nearly correspond to an inhomogeneous region of g = 50 nm.

For the case of the negative inhomogeneous field $(c_1 = -6, c_2 = -7, t_{\text{delay-c1},2} = 0 \text{ and } \beta = -0.001)$, we see that the laser intensity along the negative x direction is higher than that along the positive x direction, as shown in Figure 5(a). Based on the above illustrations, when the electron is ionized around t = 0, it will obtain more energy when it accelerates along the negative x direction from t = 0to t = 2T, where is in the A_4 region. Thus, the larger emitted photon energy can be found from P_4 , as shown in Figure 5(b), which can lead to the harmonic cutoff extension. For the case of the positive inhomogeneous field $(c_1 = -6, c_2 = -7, t_{\text{delay}-c_1} = -0.6\text{T}, t_{\text{delay}-c_2} = -0.3\text{T} \text{ and}$ β = 0.001), the higher laser enhancement along the positive x direction can be found, as shown in Figure 5(c). That is to say, when the electron is ionized around t = 0, the extra energy will be obtained during its accelerated process along the positive x direction from t = 0 to t = 1.5T, where is in the A_5 region. Therefore, the extension of P_5 can be found and it is responsible for the harmonic cutoff extension, as shown in Figure 5(d). Of course, as the inhomogeneous parameter increases, the larger harmonic cutoff can be obtained, as shown in Figure 6. However, for the convenience of discussion and calculation, we still choose

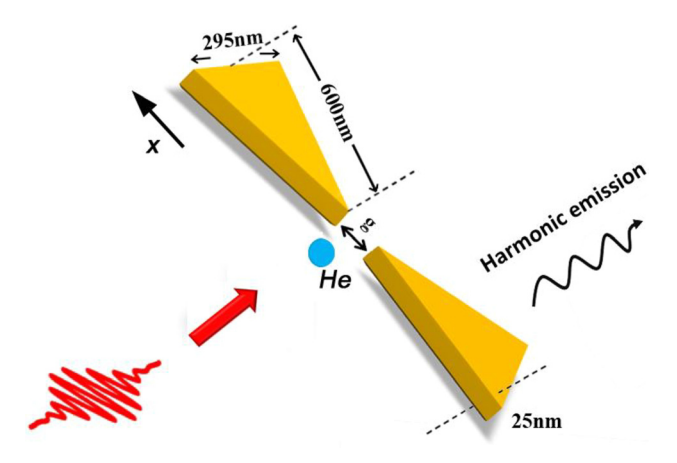


Figure 4: Schematic illustration of an inhomogeneous field and harmonic emission using a nanostructure of bow-tie elements.

 $\beta = \pm 0.001$ as the proper inhomogeneous parameters in the following discussion.

3.2 Control of the ionization process for the harmonic intensity enhancement

As discussed before, the cost of the harmonic extension is the reduction of the harmonic intensity. Thus, in this part, we try to control the ionization process to enhance the harmonic intensity. In the introduction part, we discuss some methods to improve the harmonic intensity of atomic HHG. In there, the basis point is to increase the ionization probability. However, preparing the high Rydberg state or the superposition state are a little bit difficult in the experiment. Thus, using the UV resonance ionization seems an effective method to improve the harmonic intensity. Here, the chosen gas is He atom, thus, the wavelength of the UV pulses are chosen to be $\lambda_{\rm UV}$ = 61.5, 123, 184.5 and 246 nm, which meet the single-photon, doublephoton, three-photon and four-photon resonance transition energy between the ground state and the first excited state of He atom [48]. The pulse duration and the laser intensity of the UV pulse are 1.5 fs and 0.5×10^{14} W/cm². The time delay of the UV pulse is defined as $t_{\text{delay-UV}}$.

For the case of the negative half-cycle laser profile, the time delay of the UV pulse is chosen to be $t_{delay-IIV} = 0$. As can be seen, with the introduction of the UV pulse, the harmonic intensity of the combined field can be improved by 3~4 orders of magnitude compared with the TCP, as shown in Figure 7(a). Moreover, the single-photon and double-photon UV resonance ionizations (with λ_{UV} = 61.5 and 123 nm) are much better for producing the higher intensity harmonic spectra. For the case of the positive halfcycle laser profile, the time delay of the UV pulse is chosen to be $t_{\text{delay-UV}} = -0.6\text{T}$. Clearly, as the UV pulse introduced, the harmonic intensity of the combined field can also be enhanced by 3~4 orders of magnitude in comparison with the TCP, as shown in Figure 7(b). Of course, the higher harmonic intensity from the single-photon and doublephoton UV resonance ionizations can also be found.

Figure 8 shows the laser profiles and the ionization probabilities for the cases of the three-color combined fields. For the cases of the negative and positive half-cycle laser profiles, the main body of the UV pulses cover t = 0and t = -0.6T regions, respectively (see Figure 8(a) and 8(c)). Thus, when He atom interacts with the laser field, the electron will first absorb the UV photon and jump to the excited state. Then, the electron can be ionized from the excited state. Thus, the ionization probability of the combined pulse can be remarkably increased due to the UV

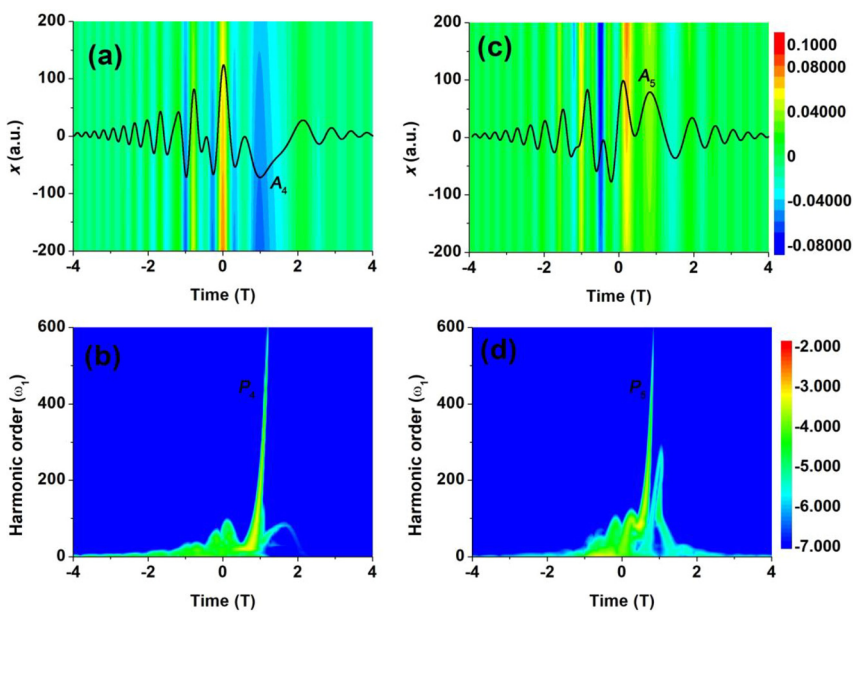


Figure 5: The time-space profile of (a) the negative half-cycle profile and (c) the positive half-cycle profile. The inhomogeneous parameters are chosen to be $\beta = -0.001$ and $\beta = 0.001$, respectively. The time profiles of high-order harmonic generation (HHG) for the cases of (b) the negative half-cycle profile and (d) the positive half-cycle profile.

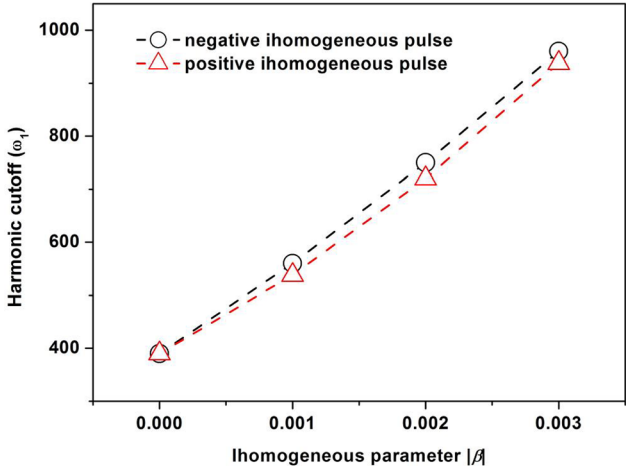


Figure 6: The inhomogeneous parameter effect on the harmonic cutoff extension.

resonance enhanced ionization [48], as shown in Figure 8(b) and 8(d). As we know that the harmonic intensity is dependent on the ionization probability. Thus, the higher ionization probability leads to the stronger harmonic intensity. Moreover, we see that the ionization probabilities from the single-photon and double-photon UV resonance ionizations are larger than those from the three-photon and four-photon UV resonance ionizations, which means the single-photon and double-photon UV resonance ionizations play the much more important role in the UV resonance ionization and the harmonic yield enhancement.

Through the combination control of the ionization and acceleration processes shown in Section 3.1 and Section

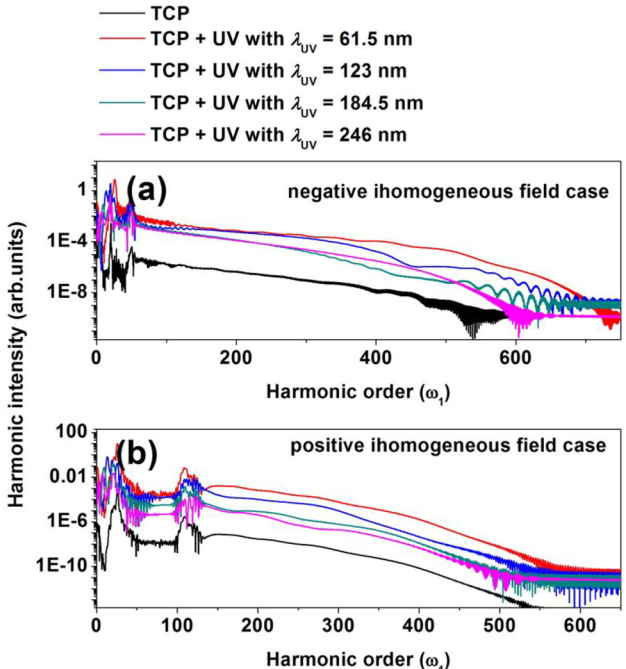


Figure 7: The high-order harmonic generation (HHG) spectra of the two-color pulse (TCP) and TCP + ultraviolet (UV) pulse (a) the negative half-cycle profile case and (b) the positive half-cycle profile case. The pulse duration and laser intensity of UV pulse are 1.5 fs and 0.5×10^{14} W/cm². The wavelength of the UV pulses are chosen to be $\lambda_{\rm UV} = 61.5$ nm, 123 nm, 184.5 nm and 246 nm. The time delays of the UV pulses are chosen to be $t_{\rm delay-UV} = 0$ and $t_{\rm delay-UV} = -0.6$ T for the above two cases, respectively.

3.2, the broader and stronger harmonic spectral plateaus with the larger harmonic cutoff can be obtained, as shown in Figure 7(a) and 7(b) for the cases of the optimal negative

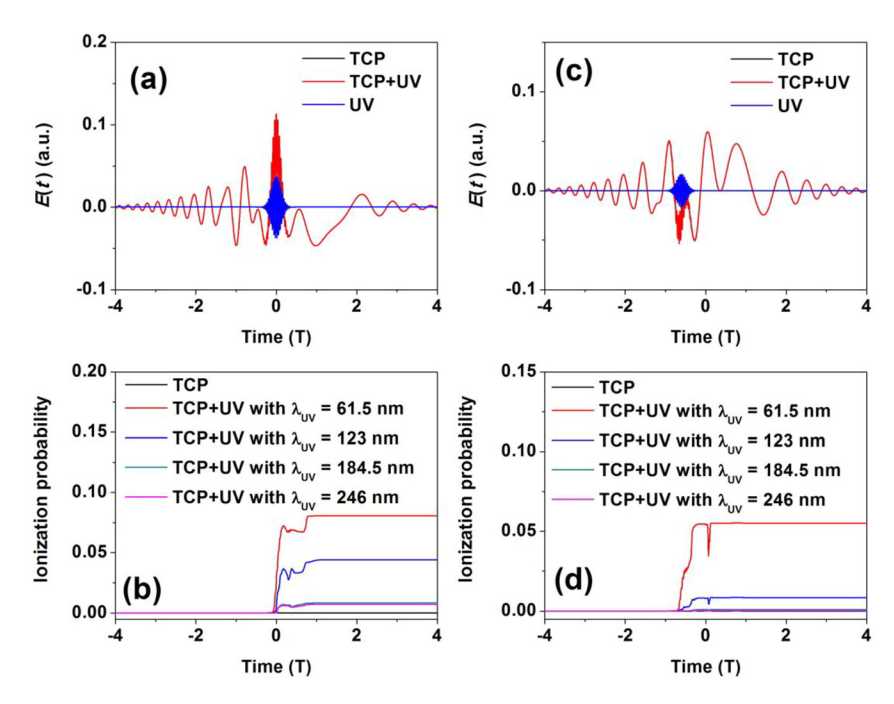


Figure 8: The laser profiles of two-color pulse (TCP), ultraviolet (UV) pulse and TCP + UV pulse for the cases of (a) the negative half-cycle profile and (c) the positive half-cycle profile. The ionization probabilities of He driven by the TCP + UV combined pulse (b) the negative half-cycle profile case and (d) the positive half-cycle profile case. Here, the UV pulse is only chosen to be 61.5 nm.

and positive half-cycle laser profiles. Moreover, through analyzing the time-profiles of HHG from the combined fields (the UV pulse is chosen to be 61.5 nm) shown in Figure 9(a) and 9(c), we see that when the harmonic spectral regions are (i) from 200th order to 600th order for the negative half-cycle laser profile case or (ii) from 300th order to 500th order for the positive half-cycle laser profile case, only the single HEP is found to contribute to the harmonic spectral plateau, which is beneficial to produce the SAPs. Therefore, by superposing the harmonics (i) from 200th order to 600th order (for the negative half-cycle laser

profile case) or (ii) from 300th order to 500th order (for the positive half-cycle laser profile case) with the harmonic width of 100 orders, a series of SAPs shorter than 45 as can be obtained, as shown in Figure 9(b) and 9(d), respectively. It should be noted that for most of the cases, when the 100 order harmonics are superposed, the single 38 as pulse can be obtained, as shown in Figure 9(b) and 9(d). However, for the case of the negative half-cycle profile, when the superposed harmonic region is from 400th order o 500th order, a 45 as pulse consisting of a main pulse and a secondary pulse can be obtained [see Figure 9(b)]. Here, if we

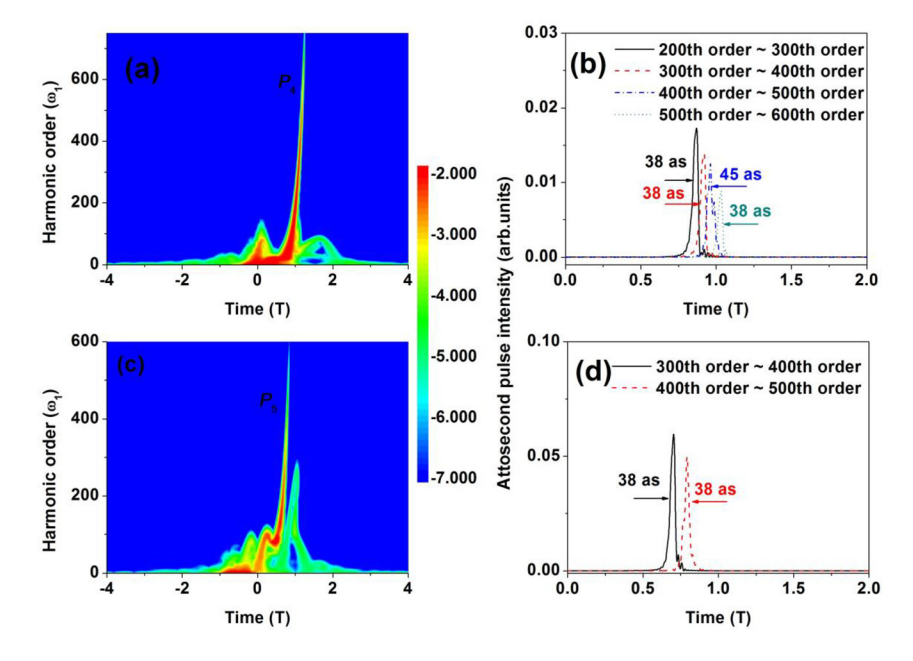


Figure 9: The time profiles of high-order harmonic generation (HHG) driven by the two-color pulse (TCP) + ultraviolet (UV) combined pulse (a) the negative half-cycle profile case and (c) the positive half-cycle profile case. The temporal profiles of the SAPs obtained from (b) the negative half-cycle combined laser profile case and (d) the positive half-cycle combined laser profile case. Here, the UV pulse is still chosen to be 61.5 nm.

measure the pulse duration of the main pulse, it is still the 38 as pulse. Thus, we think the secondary pulse is coming from the phase mismatch of some harmonics.

4 Conclusion

In conclusion, an effective method to simultaneously control the ionization and acceleration processes of HHG has been proposed. The controlling scheme includes three steps. In the first step, with the introduction of the chirps and chirp delays of the TCP, the optimal harmonic extension from the negative and positive half-cycle laser profiles can be obtained. In the second step, by properly adding the asymmetric inhomogeneous effect, the harmonic cutoffs from the negative and positive half-cycle laser profiles can be further extended. In the third step, by proper adding the UV pulse, the harmonic intensity can be improved by 3~4 orders of magnitude due to the UV resonance ionization. Moreover, the single-photon and double-photon UV resonance ionizations play the much more important role in the UV resonance ionization and harmonic yield enhancement. Finally, the stronger attosecond pulses shorter than 45 as can be obtained.

Acknowledgments: This work was supported by the Natural Science Foundation of Liaoning province, China (No. 2019-MS-167).

Author contribution: All the authors have accepted responsibility for the entire content of this submitted manuscript and approved submission.

Research funding: None declared.

Conflict of interest statement: The authors declare no conflicts of interest regarding this article.

References

- [1] F. Krausz and M. Ivanov, "Attosecond physics," Rev. Mod. Phys., vol. 81, p. 163, 2009.
- [2] M. Hentschel, R. Kienberger, C. Spielmann, et al., "Attosecond metrology," Nature, vol. 414, p. 509, 2001.
- [3] H. Liu and A. Y. Feng, "Selection and enhancement of the single harmonic emission event in the water window region," Z. Naturforsch. A, vol. 73, p. 985, 2018.
- [4] G. T. Zhang, "Intense isolated ultrashort attosecond pulse generation in a multi-cycle three-colour laser field," Z. Naturforsch. A, vol. 69, p. 673, 2014.
- [5] Y. H. Wang, C. Yu, Q. Shi, et al., "Reexamination of wavelength scaling of harmonic yield in intense midinfrared fields," Phys. Rev. A, vol. 89, 2014, Art no. 023825.
- [6] L. Li, M. Zheng, R. L. Q. Feng, and Y. Qiao, "Waveform control in generations of intense water window attosecond pulses via

- multi-color combined field," Int. J. Mod. Phys. B, vol. 33, p. 1950130, 2019.
- [7] K. J. Yuan and A. D. Bandrauk, "Single circularly polarized attosecond pulse generation by intense few cycle elliptically polarized laser pulses and terahertz fields from molecular media," Phys. Rev. Lett., vol. 110, 2013, Art no. 023003.
- [8] D. A. Telnov and S. I. Chu, "Effects of multiple electronic shells on strong-field multiphoton ionization and high-order harmonic generation of diatomic molecules with arbitrary orientation: An all-electron time-dependent density-functional approach," Phys. Rev. A, vol. 80, 2009, Art no.043412.
- [9] S. C. Jiang, J. G. Chen, H. Wei, C. Yu, R. F. Lu, and C. D. Lin, "Role of the transition dipole amplitude and phase on the generation of odd and even high-order harmonics in crystals," Phys. Rev. Lett., vol. 120, p. 253201, 2018.
- [10] Y. T. Zhao, X. Q. Xu, S. C. Jiang, X. Zhao, J. G. Chen, and Y. J. Yang, "Cooper minimum of high-order harmonic spectra from an MgO crystal in an ultrashort laser pulse," Phys. Rev. A, vol. 101, 2020, Art no.033413.
- [11] P. B. Corkum, "Plasma perspective on strong field multiphoton ionization," Phys. Rev. Lett., vol. 71, p. 1994, 1993.
- [12] J. G. Chen, R. Q. Wang, Z. Zhai, et al., "Collective-mode dynamics in a spin-orbit-coupled Bose-Einstein condensate," Phys. Rev. A, vol. 86, 2012, Art no.033417.
- [13] J. G. Chen, YJ Yang, J. Chen, and B. Wang, "Self-organized correlations lead to explosive synchronization," Phys. Rev. A, vol. 91, 2015, Art no.043403.
- [14] J. G. Chen, S. L. Zeng, Y. J. Yang, and H. Q. Liang, "Generation of intense isolated sub-40-as pulses from a coherent superposition state by quantum path control in the multicycle regime," Phys. Rev. A, vol. 83, 2011, Art no.023401.
- [15] L. Q. Feng and T. S. Chu, "Intensity improvement in the attosecond pulse generation with the coherent superposition initial state," Phys. Lett. A, vol. 376, p. 1523, 2012.
- [16] K. Ishikawa, "Photoemission and ionization of He+ under simultaneous irradiation of fundamental laser and high-order harmonic pulses," Phys. Rev. Lett., vol. 91, 2003, Art no.043002.
- [17] P. C. Li, X. X. Zhou, G. L. Wang, and Z. X. Zhao, "Isospin splitting of the nucleon-nucleus optical potential," Phys. Rev. A, vol. 80, 2009, Art no.053825.
- [18] T. Zuo, S. Chelkowski, and A. D. Bandrauk, "Harmonic generation by theH2+molecular ion in intense laser fields," Phys. Rev. A, vol. 48, p. 3837, 1993.
- [19] B. N. Wang, L. X. He, F. Wang, et al., "Resonance enhanced highorder harmonic generation in H2+ by two sequential laser pulses," Opt. Express, vol. 25, p. 17777, 2017.
- [20] L. Q. Feng, "Molecular harmonic extension and enhancement from H2+ ions in the presence of spatially inhomogeneous fields," Phys. Rev. A, vol. 92, 2015, Art no.053832.
- [21] C. Jin, A. T. Le, and C. D. Lin, "Retrieval of target photorecombination cross sections from high-order harmonics generated in a macroscopic medium," Phys. Rev. A, vol. 79, 2009, Art no.053413.
- [22] Z. N. Zeng, Y. Cheng, X. H. Song, R. X. Li, and Z. Z. Xu, "Generation of an extreme ultraviolet supercontinuum in a two-color laser field," Phys. Rev. Lett., vol. 98, p. 203901, 2007.
- [23] X. L. Ge, C. L. Xia, and X. S. Liu, "First Report of Tomato mosaic virus Infecting Pepino in China," Laser Phys., vol. 22, p. 1704, 2012.

- [24] P. F. Lan, P. X. Lu, W. Cao, Y. H. Li, and X. L. Wang, "Carrierenvelope phase-stabilized attosecond pulses from asymmetric molecules," Phys. Rev. A, vol. 76, 2007, Art no.011402.
- [25] Y. Li, L. Q. Feng, and Y. Qiao, "Selective enhancement of singleorder and two-order harmonics from He atom via two-color and three-color laser fields," Chem. Phys., vol. 527, p. 110497, 2019.
- [26] L. Q. Feng and T. S. Chu, "Generation of an isolated sub-40-as pulse using two-color laser pulses: combined chirp effects," Phys. Rev. A, vol. 84, 2011, Art no. 053853.
- [27] Y. Li, L. Q. Feng, and Y. Qiao, "Improvement of high-Order harmonic generation via controlling multiple accelerationrecombination process," Z. Naturforsch. A, vol. 74, n. 561, 2019.
- [28] H. Yuan, L. Fang, and L. Hua, "Control of high-order harmonic generation with chirped inhomogeneous fields," J. Opt. Soc. Am. B, vol. 34, p. 2390, 2017.
- [29] J. J. Carrera, and S. I. Chu, "Extension of high-order harmonic generation cutoff via coherent control of intense few-cycle chirped laser pulses," Phys. Rev. A, vol. 75, 2007, Art no. 033807.
- [30] K. Zhao, Q. Zhang, M. Chini, Y. Wu, X. W. Wang, and Z. H. Chang, "Tailoring a 67 attosecond pulse through advantageous phasemismatch," Opt. Lett., vol. 37, p. 3891, 2012.
- [31] Q. B. Zhang, P. X. Lu, P. F. Lan, et al., "Multi-cycle laser-driven broadband supercontinuum with a modulated polarization gating," Opt. Express, vol. 16, p. 9795, 2008.
- [32] G. Sansone, E. Benedetti, F. Calegari, et al., "Isolated singlecycle attosecond pulses," Science, vol. 314, p. 443, 2006.
- [33] S. Kim, J. Jin, Y. J. Kim, et al., "High-harmonic generation by resonant plasmon field enhancement," Nature (London), vol. 453, p. 757, 2008.
- [34] M. F. Ciappina, J. A. Pérez-Hernández, A. S. Landsman et al., "Attosecond physics at the nanoscale," Rep. Prog. Phys., vol. 80, 2017, Art no. 054401.
- [35] I. Yavuz, Y. Tikman, and Z. Altun, "High-order-harmonic generation from H2+molecular ions near plasmon-enhanced laser fields," Phys. Rev. A, vol. 92, 2015, Art no. 023413.
- [36] C. Yu, H. X. He, Y. H. Wang, Q. Shi, Y. D. Zhang, and R. F. Lu, "Intense attosecond pulse generated from a molecular harmonic plateau of H2+in mid-infrared laser fields," J. Phys. B: At. Mol. Opt. Phys., vol. 47, 2014, Art no. 055601.

- [37] L. Q. Feng, W. L. Li, and H. Liu, "Electron-Nuclear dynamics in molecular harmonic generation driven by a plasmonic nonhomogeneous field," Ann. Phys. (Berlin), vol. 529, p. 1700093, 2017.
- [38] R. F. Lu, P. Y. Zhang, and K. L. Han, "Attosecond-resolution quantum dynamics calculations for atoms and molecules in strong laser fields," Phys. Rev. E, vol. 77, 2008, Art no. 066701.
- [39] C. Yu, S. C. Jiang, and R. F. Lu, "High order harmonic generation in solids: a review on recent numerical methods," Adv. Phys. X, vol. 4, p. 1562982, 2019.
- [40] C. Y. Xu, L. Q. Feng, Y. Qiao, et al., "Pulse duration dependence of harmonic yield of H2+ and its isotopic molecule," Eur. Phys. J. D, vol. 74, p. 139, 2020.
- [41] H. Liu, Y. Li, H. Liu, A. Y. Feng, L. Q. Feng, and Y. Qiao, "Multipleacceleration in "W" waveform structure for high-order harmonic improvement," J. Nonlinear Opt. Phys. Mater., vol. 28, p. 1950037, 2019.
- [42] Y. Li, R. L. Q. Feng, and Y. Qiao, "Improvement of harmonic spectra from superposition of initial state driven by homogeneous and inhomogeneous combined field," Can. J. Phys., vol. 98, p. 198, 2020.
- [43] L. Q. Feng, Y. Li, and A. Y. Feng, "Nano-plasmonic-pump-probe effect on the intensity enhancement of attosecond pulse from hydrogen molecular ion," Laser Phys. Lett., vol. 15, p. 115301, 2018.
- [44] J. Hu, K. L. Han, and G. Z. He, "Correlation quantum dynamics between an electron and D2+molecule with attosecond resolution"123001, 2005.
- [45] L. Q. Feng and H. Liu, "Generation of the ultrabroad bandwidth with keV by three-color low intense mid-infrared inhomogeneous pulse," Opt. Laser Technol., vol. 81, p. 7, 2016.
- [46] P. Antoine, B. Piraux, and A. Maquet, "Time profile of harmonics generated by a single atom in a strong electromagnetic field," Phys. Rev. A, vol. 51, p. R1750, 1995.
- [47] M. F. Ciappina, S. S. Acimovic, T. Shaaran, J. Biegert, R. Quidant, and M. Lewenstein, "Enhancement of high harmonic generation by confining electron motion in plasmonic nanostrutures," Opt. Express, vol. 20, p. 26261, 2012.
- [48] L. Q. Feng and T. S. Chu, "Intensity enhancement in attosecond pulse generation," IEEE J. Quantum Electron., vol. 48, p. 1462, 2012.